PERGAMON

International Journal of Solids and Structures 38 (2001) 9267–9279

INTERNATIONAL JOURNAL OF SOLIDS and STRUCTURES

www.elsevier.com/locate/ijsolstr

Plastic deformation modes in rigid polyurethane foam under static loading

Z.H. Tu, V.P.W. Shim *, C.T. Lim

Impact Mechanics Laboratory, Department of Mechanical and Production Engineering, National University of Singapore, 10 Kent Ridge Crescent, Singapore 119260, Singapore

Received 19 July 2000; in revised form 27 July 2001

Abstract

The mechanical response of rigid polyurethane foam to compression in the rise and transverse directions was examined experimentally. Compression in the rise direction yields a three-stage stress–strain response—an initial linear elastic response leading to yield, a protracted post-yield plateau and a final sharp rise in compressive stress. Other prominent features accompanying this are strain-softening and deformation localisation. Compression in the transverse direction however, gives rise to a monotonously increasing stress–strain curve and always produces uniformly distributed deformation. This difference in deformation is attributed to anisotropy in the internal cellular structure that arises from the fabrication process. To describe deformation localisation in the foam rise direction, a simple theoretical analysis employing the concept of deformation bands is proposed. This analysis involves the parameters of deformation band thickness, band front propagation velocity, strain and strain rate within the band front, and is shown to correlate well with experiments.

Keywords: Polyurethane foam; Cellular material; Mechanical properties; Anisotropy; Deformation localisation; Deformation band

1. Introduction

Polyurethane foam materials are widely used in applications such as packaging and cushioning, and are attracting increasing attention from engineers and researchers. They are basically made of interconnected networks of solid struts and cell walls interspersed by voids or pockets with entrapped gas. Common to all foam materials are the attributes of high porosity, light weight, high crushability and good deformation energy absorption capacity. The conventional approach to describe the interconnected structure is to employ the term ''cell'' to represent the smallest structural unit. Cells are polyhedra in foams and their edges and faces are defined by struts and walls. The cell geometry (e.g. shape and size) and the way the cells are packed govern the microscopic distribution of the solid material within the cellular structure. Polyurethane foam manufactured by mixing liquid constituents and allowing them to react and expand (rise)

* Corresponding author. Tel.: +65-814-2228; fax: +65-779-1459.
E-mail address: mpespwv@nus.edu.sg (V.P.W. Shim).

0020-7683/01/$ - see front matter
PII: S0020-7683(01)00213-X

upwards exhibits normal anisotropy—cells are generally elongated in the foam rise direction due to the foaming process and this gives rise to mechanical anisotropy.

Studies on the mechanical properties of polyurethane foams are extensive and have been well documented (see e.g. Gibson and Ashby (1997) and Hilyard and Cunningham (1994)). For compression in the foam rise direction, the stress–strain relationship exhibits an initial linear rise corresponding to uniform elastic compression, followed by a protracted post-yield plateau, whereby the collapse of cells spreads through the structure. In many foam materials, compression in the foam rise direction produces a drop in stress at the beginning of the plateau phase; such behaviour is hence termed ''strain softening''. The final compression stage is signified by a steepening increase in stress as total cell collapse is completed and the compacted material begins to behave like a homogenous solid. The initial elastic phase defines the elastic modulus, yield stress and yield strain; the post-yield phase in which the stress remains nearly constant, identifies the plateau stress and densification strain. For compression transverse to the foam rise direction, the three-phase response differs slightly. There is no strain softening and the post-yield plateau is replaced by a small degree of strain hardening prior to densification. This form of mechanical behaviour facilitates the application of foam materials to damage mitigation. Micromechanical approaches (see e.g. Gibson and Ashby (1982) and Brezny and Green (1990)) have revealed correlation between the internal structure and mechanical behaviour—the mechanical properties of foam materials are functions of structural parameters (e.g. porosity, cell shape and size, strut length and thickness) and the properties of cell wall material.

The deformation of polyurethane foam is of significant relevance to practical engineering applications. For example, the high crushability of polymeric foam is a primary consideration in cushioning applications. An understanding of the deformation mechanisms is therefore important. With respect to the three phases of response for compression in the foam rise direction, the initial linear elasticity is generated by cell wall bending and cell face stretching; the plateau phase is associated with the collapse of cells by elastic buckling, formation of plastic hinges, and crushing if the cell walls are brittle. For strain-softening cellular materials, deformation is usually localised within bands. Across the band boundaries, the degree of deformation changes abruptly, characterising a discontinuity (see e.g. Vaz and Fortes (1993) and Shim et al. (2000)). Although deformation in the loading direction can be very severe, deformation transverse to this is almost negligible, i.e. Poisson's ratio is approximately zero and volume is not conserved, a contrast to continuum solids. These plastic deformation modes and mechanisms have been characterised in a number of recent studies, particularly by Bastawros and coworkers (1998, 2000) and McCullough et al. (1999), who innovatively employed X-ray imaging and surface strain mapping techniques for their investigations. The present effort examines specifically the response of a rigid polyurethane foam to uniaxial compression in both the rise and transverse directions. A simple and effective theoretical analysis pertaining to deformation localisation is formulated and is then experimentally verified.

2. Polyurethane foam and its structure

The polyurethane foam used in this study was fabricated by blending two chemical constituents—Daltofoam TP 12073 and Suprasec 5005 (Imperial Chemical Industries products), in the presence of a blowing agent. The former is a compounded polyether polyol blend and the latter a higher functionality isocyanate, both in liquid form. The blowing agent used is CFC 11 (liquid Freon), which vaporises readily to generate gas bubbles in the foaming process. The weight proportions of Daltofoam, Suprasec and CFC are 100 : 135 : 35. This produces a rigid polyurethane foam with a density of 25.6 kg/m^3. Microscopic examination of the resulting internal structure reveals that it comprises both open and closed cells, the latter accounting for the greater portion. The cell walls of closed cells are thin membranes while the cell edge struts are much thicker. The structure exhibits an anisotropic geometry—cells are generally elongated in the foam rise direction; this is evident from microscopic views in both the rise and transverse directions (Fig. 1). The average cell size is

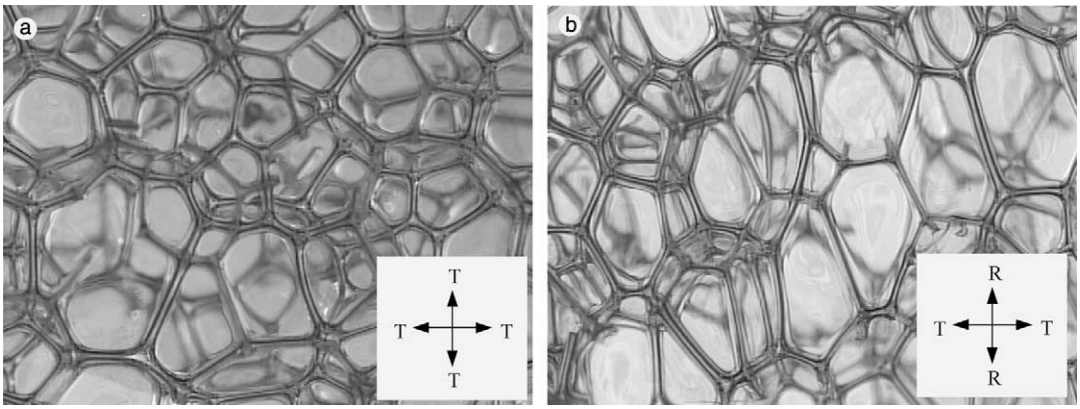

Fig. 1. Microscopic views of polyurethane foam in the (a) rise and (b) transverse directions.

about 0.71 mm in the rise direction and 0.58 mm in the transverse direction. This implies that the cross-section perpendicular to the rise direction is materially denser than that parallel to the rise direction.

3. Compression experiments

The static mechanical properties of polyurethane foam were investigated via compression and interrupted loading and reloading. These tests were carried out using an Instron universal testing machine, which can generate extension/compression rates of up to 20 cm/s and is therefore appropriate for applying quasi-static and low strain rate deformation. Experimental data in the form of force–displacement signals were recorded, digitised and transferred to a personal computer for post-processing to produce stress–strain curves. The specimens were made sufficiently large to exclude size effects.

Polyurethane foam specimens were fabricated in the form of cubes with 100 mm sides for uniaxial compression tests. Loading was applied at a rate of 5 mm/min in the rise or transverse direction. The sides of specimens were scribed with equally spaced horizontal lines to aid visualisation of deformation. A digital video camera was used to record the deformation process. Fig. 2 shows typical experimental stress–strain curves for compression in the foam rise and transverse directions and Table 1 presents the values of some characteristic quantities.

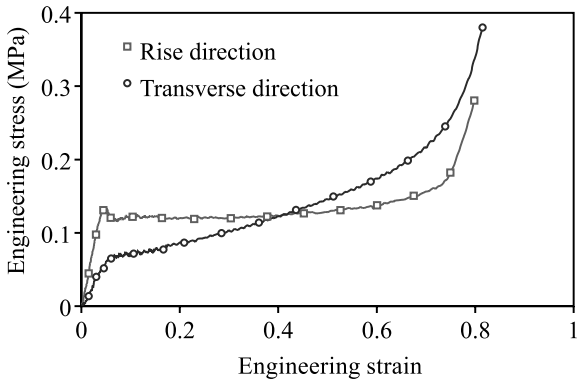

Fig. 2. Typical stress–strain curves for polyurethane foam under compression in the rise and transverse directions.

Table 1
Mechanical properties of polyurethane foam under compression

Quantities	Rise direction	Transverse direction
Young's modulus (MPa)	2.78	1.30
Yield stress (MPa)	0.15	0.07
Yield strain (%)	5.4	6.2
Plateau stress (MPa)	0.12	NA
Strain at onset of densification (%)	80	75

The stress–strain response shows that compression in the foam rise direction engenders the three characteristic phases—an initial linear elastic response leading to yield, a protracted post-yield plateau and a final sharp rise in compressive stress (Fig. 2). As stated earlier, such behaviour is common in cellular materials. A prominent feature is the small drop in stress at the commencement of the plateau phase—strain softening. The roughly constant stress plateau comprises minute fluctuations about a level of 120 kPa; these fluctuations are peculiar to the response of many cellular structures. The yield strain defining the end of initial elasticity and the densification strain signifying the end of the stress plateau were found to be 5.4% and about 80% respectively.

Response to compression transverse to the rise direction is quite different. There is no plateau phase and no strain softening is observed. The stress initially increases linearly to the yield point, which is about half the yield stress for the rise direction; thereafter it continues to climb at a more gradual rate until it achieves a final steep rise, similar to that for compression in the rise direction. The curve intersects with that for the rise direction at a strain of about 0.4 and assumes a value approximately 30% higher than the latter at the densification strain (Fig. 2). Experimental results show that the Young's modulus and yield stress in the transverse direction are about half their values in the rise direction, while the yield strain is slightly larger. The differences in response for the two directions show that the mechanical properties of polyurethane foam are direction dependent and arise from microstructural anisotropy.

Visual inspection of specimens reveals that compression in the foam rise direction causes narrow localised deformation bands, while deformation is uniformly distributed for compression in the transverse direction (Fig. 3). Post-yield compression in one direction however, induces negligible deformation in the other. Consequently, attention is focused on deformation in the direction of loading.

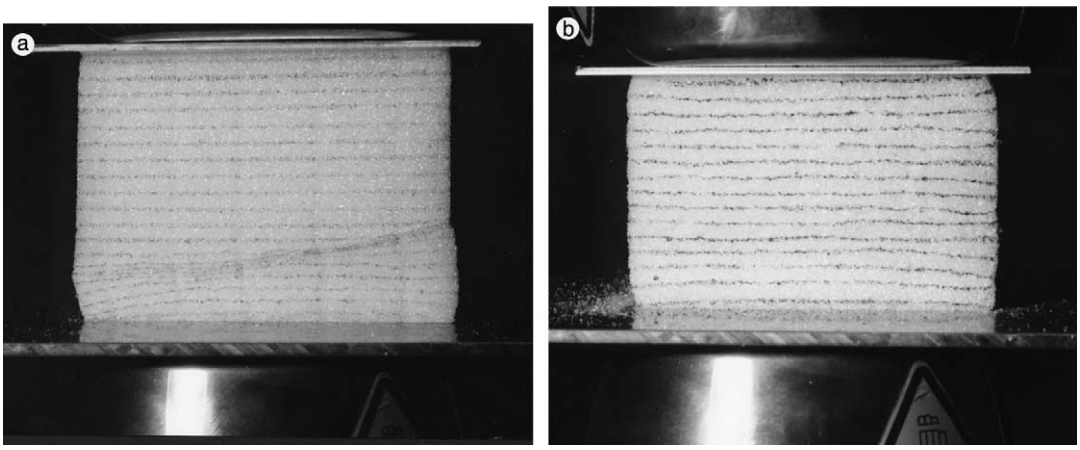

Fig. 3. Deformation of polyurethane foam for compression in the (a) rise and (b) transverse directions.

4. Analysis of deformation

In the tests, deformation associated with compression in the foam rise direction is not uniform within the specimen but is localised in narrow bands. This section describes the response observed using the concept of deformation bands and analysis is restricted to deformation in the foam rise direction.

4.1. Mechanism of deformation

Compression in the foam rise direction gives rise to the three phases of response described, each corresponding to distinct deformation mechanisms. The initial linear elasticity is controlled by elastic axial compression and bending of cell edges, stretching of cell faces and compression of gas within closed cells. Deformation during this phase is small and uniformly distributed throughout the specimen. In the protracted plastic plateau phase, cells collapse via buckling, plastic deformation or rupture of cell walls and edges. Deformation in this stage is not uniformly distributed and accounts for the major portion of the global response. Final densification is associated with completely collapsed cells being compacted against one another. Deformation again is uniformly distributed and the stress rises steeply as solid cell wall material is pressed together.

The non-uniformly distributed deformation in the plateau phase is a feature peculiar to strain-softening cellular materials. A block of foam can be considered to be composed of many cell layers, each possessing a slightly different yield strength. Commencement of the plateau phase arises from failure of the weakest cell layer. Since there is a decrease in the post-yield stress due to buckling of cell walls, gross deformation is localised within this layer until the voids contained are eliminated and the collapsed cell walls are compacted against each other. Collapse of this layer weakens the adjacent layers, thus making them the next most susceptible to collapse. Consequently, localised deformation spreads to the adjacent layer and a subsequent cycle of confined collapse is triggered. Repetition of this cycle results in the propagation of localised deformation through the elastic region and eventually leads to complete collapse of the whole block of material, thus signifying the end of the plateau phase.

4.2. Deformation band and band front

The significant feature during the plateau phase is that deformation is not uniformly distributed throughout. There are three different regions of deformation—elastic, collapsing and collapsed. However, deformation within each region is homogenous. Denoting the yield and the densification strains by ε_y and ε_d, the strain within the elastic region is ε_y, while it is ε_d in the collapsed region and has an intermediate value between ε_y and ε_d in the collapsing zone. The concept of a deformation band is somewhat similar to that of Luders band for metallic materials (see e.g. Hall (1970)) and has been employed by Vaz and Fortes (1993) in an effort to characterise the deformation regions described. A deformation band refers to a collapsed region and a band front is the boundary that separates the elastic and collapsed zones (Fig. 4). Therefore, the strain in the band is ε_d and that in the band front lies between ε_y and ε_d. It is also possible that at any instant, there are multiple bands and band fronts.

Gross deformation comprises the formation and propagation of deformation bands. Initially, the material is completely elastic and no bands exist. Under compression, the weakest cell layer yields, generating a band front. Gross deformation is confined within the band front until complete collapse of cells occurs. The collapsed layer thereby evolves into a deformation band and the band front moves one layer forward to the adjacent layer, which eventually adds to the band after it collapses. This cycle of events is repeated and the band front travels through the elastic region, resulting in expansion of the deformation band at the cost of the elastic zone. During the plateau phase, gross deformation is restricted to the band front—the collapsed band and the elastic region essentially do not contribute to gross deformation. Vaz and Fortes (1993)

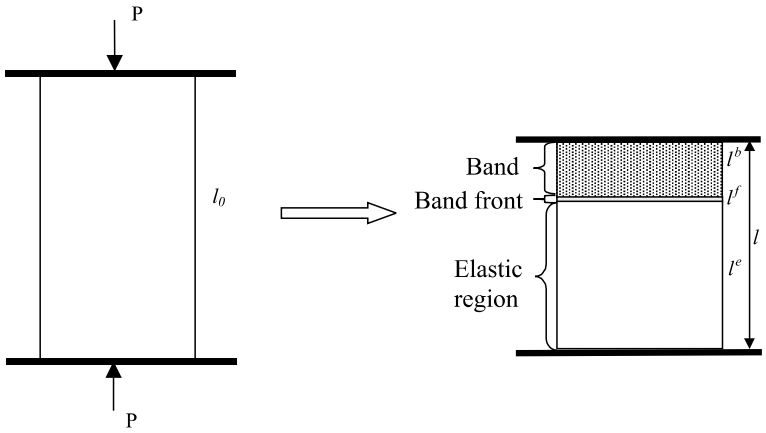

Fig. 4. Schematic representation of the three deformation regions in a specimen under uniaxial compression.

examined a rigid foam and experimentally obtained the band velocity, the strain rate within the band front and several other parameters relating to the band. He found that experimental results for the case of a single band yielded good agreement with values calculated using formulae for Luders bands (see e.g. Hahn (1962) and Doncel et al. (1995)).

Instead of assuming the analysis established for Luders bands at the outset, the present effort develops a set of simple theoretical expressions specifically for foam material, to identify deformation band thickness, thickness of a band front, its propagation velocity and the strain rate within a band front. Relevant parameters are also identified for multi-band cases.

4.3. Thickness of deformation band and band front

The thickness of both the deformation band and the band front can be determined for the case of a single band. To facilitate the present analysis, it is assumed that the band front travels in the direction of compression; this is the case for many cellular materials. Care should be exercised, because for a rigid polyurethane foam, this assumption is not always strictly true (e.g. Fig. 3(a), where the deformation band expands both upwards and downwards). Consider a block of polymeric foam subjected to uniaxial compression. The block has an initial height l_0 and deforms to a height of l (Fig. 4).

The global strain ε (engineering stresses and strains are used throughout the analysis) is thus:

$$\varepsilon = 1 - \frac{l}{l_0} \tag{1}$$

The thicknesses of the deformation band, band front and elastic region are denoted by l^{b}, l^{f} and l^{e} respectively. The band front is a single cell layer and thus its thickness is equal to the average cell size (less than 1 mm for polyurethane foam). Hence, l^{f} is negligible compared with l^{e} and l^{b}, resulting in the approximate relation:

$$l = l^{\mathrm{e}} + l^{\mathrm{b}} = (1 - \varepsilon) l_0 \tag{2}$$

As stated previously, the strain in the elastic region is ε_{y} and that in the deformation band is ε_{d}. Denoting the initial (undeformed) thickness of the current elastic zone as l_0^{e} and the initial thickness of the deformation band as l_0^{b}, the current strains in these zones are thus:

$$\varepsilon_y = 1 - \frac{l^e}{l_0^e} \tag{3}$$

$$\varepsilon_d = 1 - \frac{l^b}{l_0^b} \tag{4}$$

From the preceding two equations, the original material thickness can be expressed in terms of ε_y and ε_d:

$$l_0 = l_0^e + l_0^b = \frac{l^e}{(1-\varepsilon_y)} + \frac{l^b}{(1-\varepsilon_d)} \tag{5}$$

Solving Eqs. (2) and (5) for l^e and l^b yields the current thicknesses of the elastic zone and the deformation band in terms of the global strain ε and the strain parameters ε_y and ε_d which characterise the material under investigation:

$$l^e = \frac{(1-\varepsilon_y)(\varepsilon-\varepsilon_d)}{\varepsilon_y - \varepsilon_d} l_0 \tag{6}$$

$$l^b = \frac{(1-\varepsilon_d)(\varepsilon-\varepsilon_y)}{\varepsilon_d - \varepsilon_y} l_0 \tag{7}$$

Variation of the dimensionless thickness of the deformation band and elastic zone with global deformation (engineering strain) is shown in Fig. 5. In reality, ε_y is much smaller than ε_d and is therefore negligible. This reduces the preceding expressions to:

$$l^e = -\frac{\varepsilon-\varepsilon_d}{\varepsilon_d} l_0 \tag{8}$$

$$l^b = \frac{(1-\varepsilon_d)\varepsilon}{\varepsilon_d} l_0 \tag{9}$$

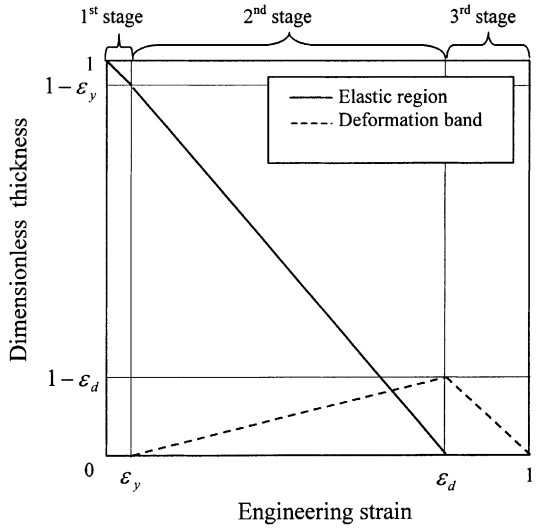

Fig. 5. Variation of dimensionless deformation band and elastic region thickness with global strain.

This analysis is based on the assumption that ε_y and ε_d remain constant during loading. Eqs. (8) and (9) enable an estimate of the thickness of the deformation band and the elastic region for a given strain. These values have practical significance, as the current size of the elastic portion usually defines the remaining energy absorption capacity of cellular materials (see e.g. Stupak and Donovan (1994)).

4.4. Band front propagation velocity

The propagation velocity of the band front is obtained by taking the time derivative of l^e, i.e. $-\mathrm{d}l^e/\mathrm{d}t$ (with reference to Fig. 4). Hence, from Eq. (6),

$$v_b = \frac{(1-\varepsilon_y)\dot{\varepsilon}}{\varepsilon_d - \varepsilon_y} l_0 \tag{10}$$

where v_b is the band front propagation velocity. Eq. (10) shows that v_b is a function of the global strain rate. If the global compression rate of the material is v, the accompanying global strain rate can be determined from:

$$\dot{\varepsilon} = \frac{v}{l_0} \tag{11}$$

Eqs. (10) and (11) yield the relationship between v_b and v:

$$v_b = \frac{1-\varepsilon_y}{\varepsilon_d - \varepsilon_y} v \tag{12}$$

If ε_y is negligible, the preceding expression simplifies to a linear relationship between the band front propagation velocity and the global compression rate.

$$v_b = \frac{v}{\varepsilon_d} = \frac{\dot{\varepsilon}}{\varepsilon_d} l_0 \tag{13}$$

This expression is similar to that derived for Luders bands in metallic materials (Hahn, 1962) and shows that the band front propagation velocity is greater than that of the global compression rate.

4.5. Strain and strain rate within the band front

During the plateau phase (i.e. second stage of the compression response) gross deformation is essentially confined within the band front. This begs the question of what the strain and strain rate in the band front are. Recall that the undeformed thickness of a band front is the average cell size, D. Over an infinitesimal time increment $\mathrm{d}t$, the change in the overall height of the specimen is $v\,\mathrm{d}t$. This change is attributed totally to deformation in the band front and hence the strain increment within the band front is:

$$\mathrm{d}\varepsilon_b = \frac{v\,\mathrm{d}t}{D} \tag{14}$$

The strain rate in the band front is thus:

$$\dot{\varepsilon}_b = \frac{v}{D} \tag{15}$$

Since D is much smaller than l_0, the strain rate within the band front is consequently much higher than the global strain rate.

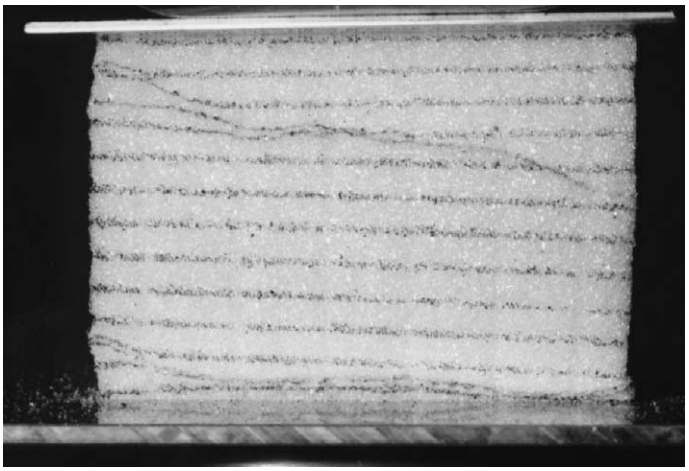

Fig. 6. Two deformation bands within a specimen.

4.6. Multi-band cases

It is expected that more than one band might be formed during the crushing of a foam specimen. This is because actual cells are randomly arranged and vary in size, shape, orientation and strength. Also, defects such as missing walls and larger voids are commonly introduced during material fabrication. As a result, two or more bands may be generated simultaneously or successively within a specimen; one example is shown in Fig. 6. Moreover, a band which is not initiated adjacent to the upper or lower rigid boundaries, but in a layer within the material specimen, will have two band fronts which will propagate from both interfaces with the upper and lower neighbouring elastic zones. This situation makes it difficult to estimate the propagation velocity of individual band fronts, but Eqs. (13) and (15) are still applicable if the left-hand side is replaced by a summation of the corresponding variable.

$$\sum_{i=1}^{m} v_{\mathrm{b}}^{(i)} = \frac{v}{\varepsilon_{\mathrm{d}}} \tag{16}$$

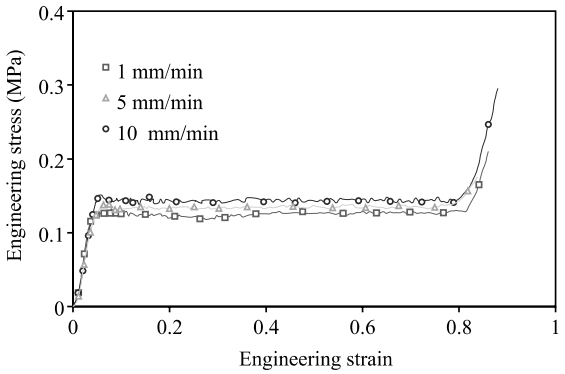

Fig. 7. Stress–strain curves for polyurethane foam under three loading rates.

Table 2
Yield and densification strains of polyurethane foam at three strain rates

Strain rate (s^{-1})	1.67×10^{-4}	8.33×10^{-4}	1.67×10^{-3}
Yield strain (%)	5.3	5.6	5.5
Densification strain (%)	82	80	80

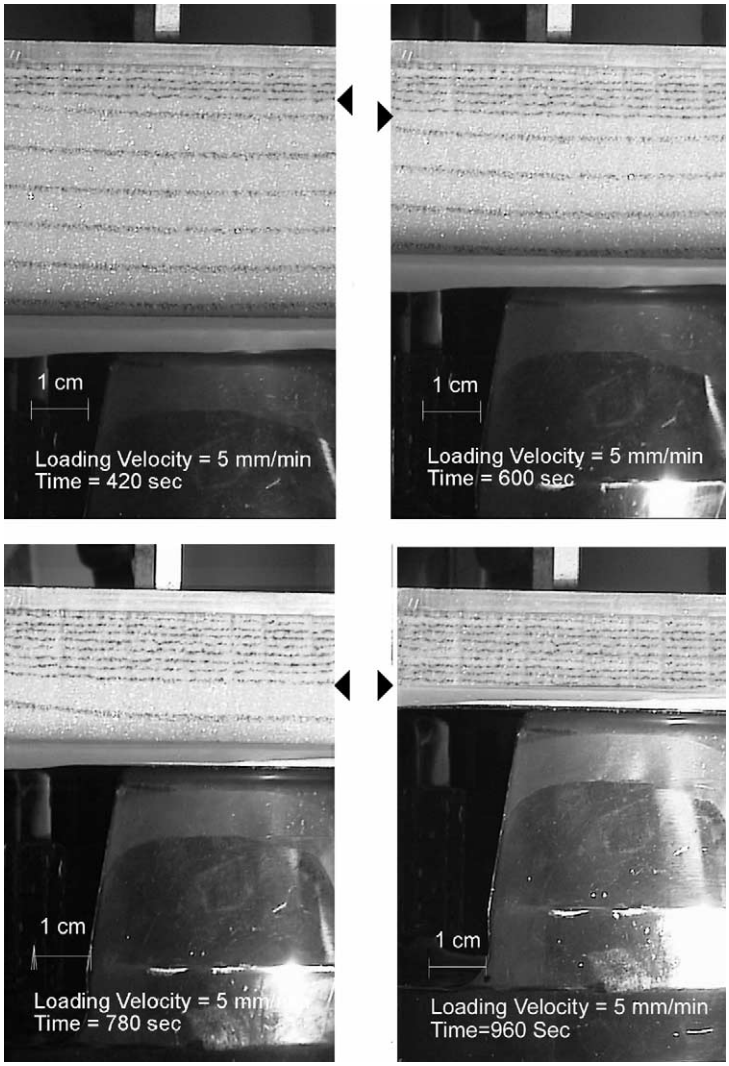

Fig. 8. Sequential photographs of the compression of polyurethane foam for a single band case.

$$\sum_{i=1}^{m} \dot{\varepsilon}_{\mathrm{b}}^{(i)} = \frac{v}{D} \tag{17}$$

where m is the number of band fronts.

4.7. Experimental verification

Low-speed uniaxial compression tests on rigid polyurethane foam were conducted to verify the expressions established. Cubic specimens with 100 mm sides were compressed at three different loading rates: 1, 5 and 10 mm/min, which correspond to global strain rates of 1.67×10^{-4}, 8.33×10^{-4} and 1.67×10^{-3} s^{-1} respectively. A digital video camera was used to record the deformation process in each specimen. The stress–strain curves for the three strain rates are shown in Fig. 7, which indicates that there is a slight increase in the stress level with strain rate, but the yield and densification strains are little affected (see Table 2).

Collapse was frequently observed to initiate in the (uppermost) layer in contact with the loading platen, as this upper surface comprises many cells with missing walls, thus making it weaker. Hence, the band front usually forms at one end of the specimen and propagates to the other. Fig. 8 is a photographic sequence illustrating the compression of a foam block. The boundary between the deformation band and the elastic region is discernible throughout the crushing process, making it possible to measure the thickness of the two zones during the plateau phase of the deformation response. The position of the band front is indicated by an arrowhead in each photograph. Fig. 9 shows comparisons between predicted and experimental results for the elastic zone and deformation band thicknesses, as functions of global strain, for the three compression rates. A comparison between the theoretical and experimental variation of band propagation velocity with global strain rate is depicted in Fig. 10. Correlation of the theoretical results with experimental data is very favourable, substantiating the validity of Eqs. (6), (7) and (10). As the yield and densification

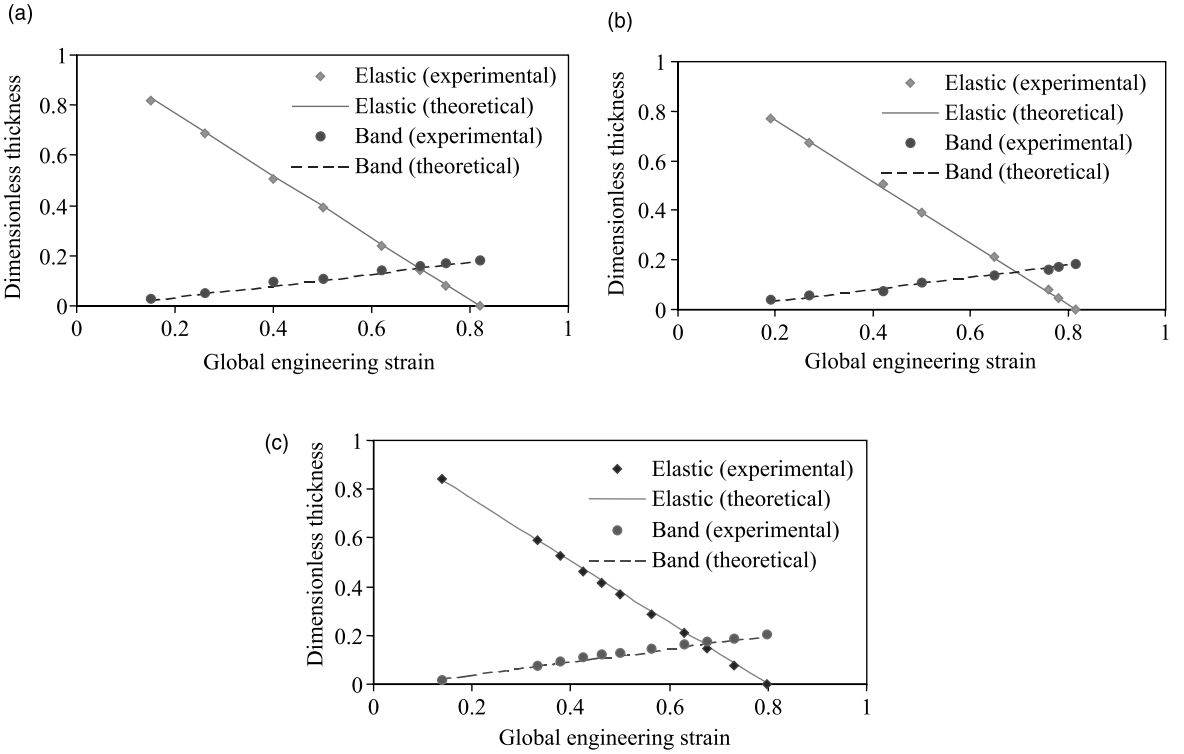

Fig. 9. Thickness of the elastic region and the deformation band for three loading rates: (a) 1 mm/min; (b) 5 mm/min and (c) 10 mm/min.

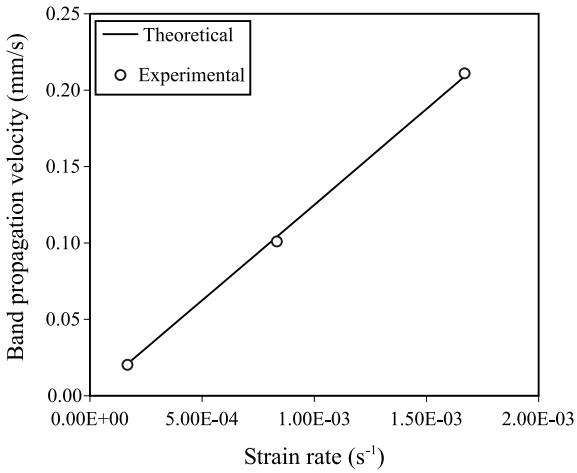

Fig. 10. Band propagation velocity at three strain rates.

strains remain essentially constant over strain rates ranging from 1.67×10^{-4} to 1.67×10^{-3} s^{-1}, this suggests that the preceding expressions are valid for this regime of strain rates.

5. Conclusions

The static mechanical properties of polyurethane foam were examined via compression in different directions and speeds. Test results show that the response is anisotropic, with the foam rise direction being stiffer and stronger. Strain softening occurs in this direction and compression yields localised deformation; compression in the transverse direction however always produces uniformly distributed deformation.

The deformation process for cellular materials has been described in terms of deformation bands. An accompanying simple theoretical analysis involving the parameters of deformation band thickness, band front propagation velocity, strain and strain rate within the band front has also been proposed. Uniaxial compression of rigid polyurethane foam at three strain rates has demonstrated the validity of the analysis. A point to be noted is that Eqs. (6) and (7) are based on the assumption that the yield and densification strains remain constant. This however may not always be the case in practice, as many cellular materials are rate sensitive. Application of the expressions derived should therefore be limited to deformation at constant strain rates or within a range of strain rates whereby the yield and densification strains vary negligibly.

References

Bart-Smith, H., Bastawros, A.F., Mumm, D.R., Evans, A.G., Sypeck, D.J., Wadley, H.N.G., 1998. Compressive deformation and yielding mechanisms in cellular Al alloys determined using X-ray tomography and surface strain mapping. Acta Mater. 46, 3583–3592.

Bastawros, A.F., Smith, H.F., Evans, A.G., 2000. Experimental analysis of deformation mechanisms in a closed-cell aluminium alloy foam. J. Mech. Phys. Solids 48, 301–322.

Brezny, R., Green, D.J., 1990. The effect of cell size on the mechanical behaviour of cellular materials. Acta Metall. Mater. 38, 2517–2526.

Doncel, G.G., Adeva, P., Cristina, M.C., Ibanez, J., 1995. Luders band formation in a rapidly solidified Ni_3Al alloy ribbon. Acta Metall. 43, 4281–4287.

Gibson, L.J., Ashby, M.F., 1997. Cellular Solids: Structure and Properties. Cambridge University Press, Cambridge.
Gibson, L.J., Ashby, M.F., 1982. The mechanics of three-dimensional cellular materials. Proc. R. Soc. Lond. A 382, 43–59.
Hahn, G.T., 1962. A model for yielding with special reference to the yield-point phenomena of iron and related bcc metals. Acta Metall. 10, 727–738.
Hall, E.O., 1970. Yield Point Phenomena in Metals and Alloys. Macmillan, London.
Hilyard, N.C., Cunningham, A., 1994. Low Density Cellular Plastics. Chapman & Hall, London.
McCullough, K.Y.G., Fleck, N.A., Ashby, M.F., 1999. Uniaxial stress–strain behaviour of aluminium alloy foams. Acta Mater. 47, 2323–2330.
Shim, V.P.W., Tu, Z.H., Lim, C.T., 2000. Two-dimensional response of crushable polyurethane foam to low velocity impact. Int. J. Impact Engng. 24, 703–731.
Stupak, P.R., Donovan, J.A., 1994. Deformation and energy absorption of polymer foams as a function of 2-D indenter and absorber geometries. Polym. Engng. Sci. 34 (10), 857–864.
Vaz, M.F., Fortes, M.A., 1993. Characterisation of deformation bands in the compression of cellular materials. J. Mater. Sci. Lett. 12, 1408–1410.